SPECTRACAM^{TM} – Random Access Charge Injection Device Cameras for Spectroscopy

Suraj Bhaskaran, Herb Ziegler, Claudia Borman, John Swab, Carey Beam, Tony Chapman, John Capogreco, Steve VanGorden, Mark Greco, Matt Pace, Zulfiqar Alam, Jon Miles, Mike Pilon, Joe Carbone
Spectra-Physics, Cameras and Imagers, Liverpool NY 13088
and
Helen Jung, Rindy Finney, Linda Lee, Victor Tsai, and Arnold London
Supertex inc, Sunnyvale CA 94089
and
Bruce Meyers
Oneida Research Services, Whitesboro NY 13492

ABSTRACT

We designed, built, and tested the SpectraCAM84/86, a family of scientific Random Access Charge Injection Device (RACID) cameras for analytical spectroscopy and quantitative imaging.

The cameras feature the RACID84/86 imagers, which are CMOS CID image sensors with true random pixel selection, integration, and readout. We developed CMOS CID technology in order to integrate high transparency RACID pixel arrays with CMOS on-chip camera circuitry. Pixels are 27-micron x 27-micron square. The RACID84 contains 1026x1026 pixels. The RACID86 has 540x540 pixels. Pixel data is read out on-chip with low noise preamplifier-per-column FETs. Image readout speed is selectable: the slow scan runs at 50kHz and the fast scan runs at 200kHz.

Dark current is reduced using a three-stage thermoelectric cooler and water recirculating system. Typical imager operating temperature is -30C to -45C. The SpectraCAM converts integrated pixel charge data into 16-bit digital output. Using nondestructive readout, the linear dynamic range of the camera is 10^7.

Spectral response extends from 165 nm to 1000 nm. RACID86 UV responsivity is 85-90 ma/watt at 350nm and 57-63 ma/watt at 200nm for illumination with an Oriel 30-watt deuterium lamp. RACID84 UV responsivity is 71-89 ma/watt at 350nm and 40-50 ma/watt at 200nm.

Keywords: CID, CMOS imaging, spectroscopy, UV sensors, scientific cameras

1. INTRODUCTION

Quantitative Imaging is the ability to take pictures and record quantitative optical information in addition to the image. From astronomy to earth science, from forensic analysis to pharmaceutical biochemistry, modern science and technology rely on the methods of quantitative imaging. To serve the needs of scientific and technical markets for quantitative imaging cameras, we designed and built the SpectraCAM84/86.

The SpectraCAM84/86 is a line of scientific cameras with true random pixel selection and integration. At the heart of the SpectraCAM is the RACID84/86 imager. The Random Access Charge Injection Device (RACID) imager is a solid-state imaging device similar to CCD and CMOS image sensors. RACID84/86 imagers are silicon CMOS integrated circuits with large area RACID pixel arrays and the associated on-chip operating circuitry.

The SpectraCAM controller uses a 16-bit gray scale to present images. The RACID exposure software is written for PENTIUM^{TM} CPU/PC104+ computer architecture. Exposure time is automatically varied from pixel to pixel on the basis of real time signal intensity. Weak signals are integrated for long periods while intense signals are integrated over several short integration cycles. This method, called Random Access Integration (RAI), makes possible the extended 10^7 linear dynamic range of the SpectraCAM. By using the RAI technique with selective region of interest clearing, weak optical signals can be captured even in the presence of very intense light sources.

2. DESIGN AND OPERATION

The RACID84/86 imagers contain X/Y addressable pixel arrays. Each pixel (picture element) contains two MOS capacitors, as shown in figure 1. Each MOS capacitor is formed between the polysilicon top electrode and the single crystal epitaxial silicon bottom electrode, separated by the SiO2 gate dielectric. One MOS capacitor is the row charge storage capacitor. It is addressed by the row circuitry. The other MOS capacitor is the column charge sense capacitor.

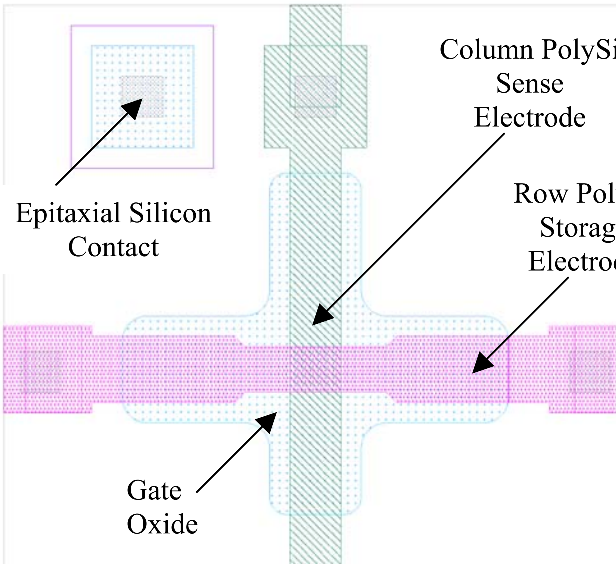

Figure 1: RACID84 Pixel MOS capacitors

The sense electrode is addressed by the column circuitry. A metal column bus connects the polysilicon sense electrodes of all pixels in one column. Another metal bus connects the polysilicon storage electrodes of all pixels in one row. The full level, 4-pixel layout of the RACID84 is shown in figure 2.

Pixel layouts use minimum allowed geometries as much as possible in order to keep the pixel transparency high. The column bus is connected to the polysilicon sense gate of a dual-gate readout FET. The sense gate of the dual-gate FET is strapped with metal to reduce the resistance of the sense gate and the associated Johnson (thermal) noise. There is one readout FET at the end of each column to integrate and amplify the charge collected in the pixels. This is called the preamplifier-per-column architecture. It was first described and implemented on PMOS CID imagers by Gerald Michon at General Electric (1-3).

Preamp-per-row (PPR) architecture is used in the PMOS CID SIcam™, a PC-based scientific instrumentation camera developed at CID Technologies (4). An off-chip summation amplifier with a feedback loop tied into each column preamplifier FET can be used to lessen the sensitivity of the output to the individual amplifier gain differences (5).

The RACID84/86 dual gate voltage amplification readout FET is shown in figure 3. Contact between the polysilicon sense gate and the metal strap is made over the field oxide region and is not shown in figure 3. The current designs use very large preamplifier MOSFETs: 800 microns Wg x 2.0 microns Lg. The preamplifier-per-column schematic is shown in figure 4.

RACID84/86 pixels are 27-micron x 27-micron squares. The 1M-pixel RACID84 is built using 2.0-micron CMOS CID technology. It contains a 1026x1026 pixel array. The RACID86 imager is built using 1.2-micron CMOS CID technology. It contains a 540x540 pixel array. The CMOS pixel control circuitry is located on two sides of the pixel array, as can be seen in figure 5.

The block diagram of the RACID84/86 is shown in figure 6. On-chip logic is designed to simplify the camera control interface. The chip architecture has six main building blocks: the serial-to-parallel shift registers, the up/down address counters, the TTL level translators, the address decoders, the address latches, and the electrode multiplexers. There are two serial ports for loading X-Y pixel address codes. Row and column addressing is accomplished with the 11-bit serial-to-parallel shift registers, address decoders, and electrode multiplexers. Vertical and horizontal latches hold the row and column addresses for all subarray functions, including pixel binning and subarray injection. User-defined regions of interest within the pixel array can be selected with independent horizontal and vertical control. Pixels in any region of interest can be binned for collective readout, in groups of pixels up to 4 columns and up to 4 rows in size. Individual pixels or groups of pixels can be chosen and read out in any order. Image readout speed is selectable: the slow scan runs at 50kHz and the fast scan runs at 200kHz.

Read noise and camera conversion gain are determined by the mean variance method (6-7). The light source used for the test is a low power 598-nm LED. The LED is positioned 15 mm behind a 500-micron diameter pinhole. A small area of 12 pixels x 12 pixels (324microns x 324microns) on the imager is selected for test. The imager is illuminated by flashing the light source for a short time, typically 1-2 msec. The resulting image is recorded and cleared.

The imager is then illuminated again, with a second flash of equal duration. The second image is subtracted from the first, to remove the spatial fixed pattern noise due to pixel-to-pixel variation in response. The resulting difference array represents the temporal noise of the system. The difference array is then averaged to obtain the mean and the standard deviation. The process is repeated for increasing exposure levels, from 1 flash to 9 flashes. The mean and standard deviation are calculated for each difference array. The variance, or square of the standard deviation of the difference array, is plotted against the signal mean, in analog-to-digital units (ADUs), as shown in figure 7. The best-fit line is calculated for the data. The slope of the resulting plot is the system gain in carriers/(ADU). The y-intercept is the square of the read noise.

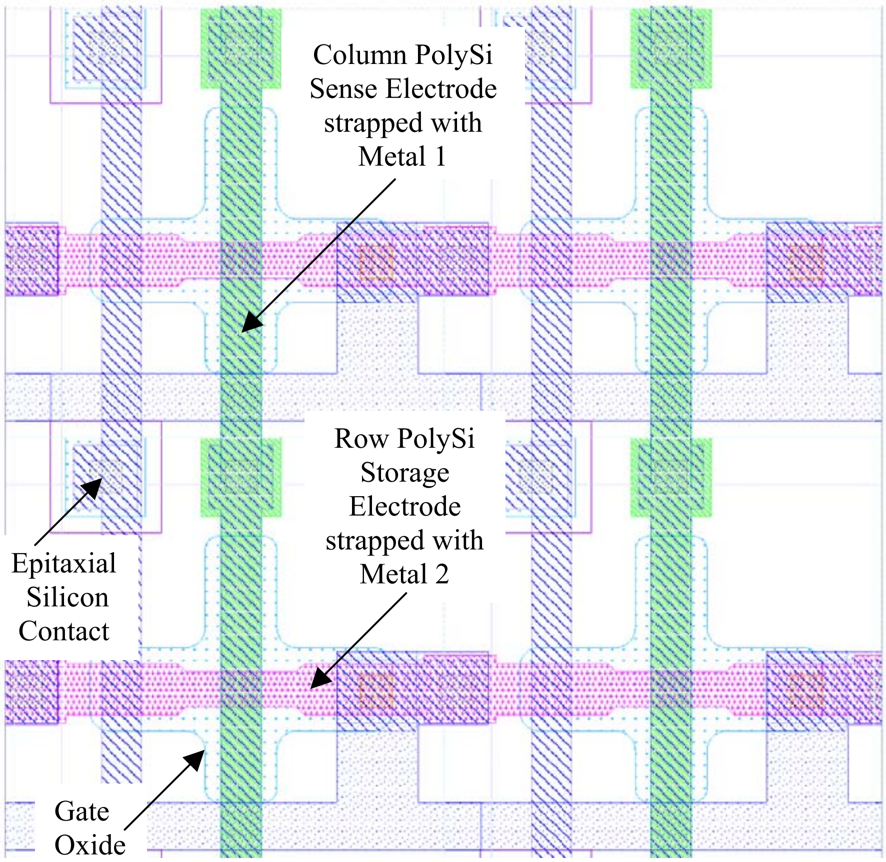

Figure 2: RACID84, full layout of 4 pixels

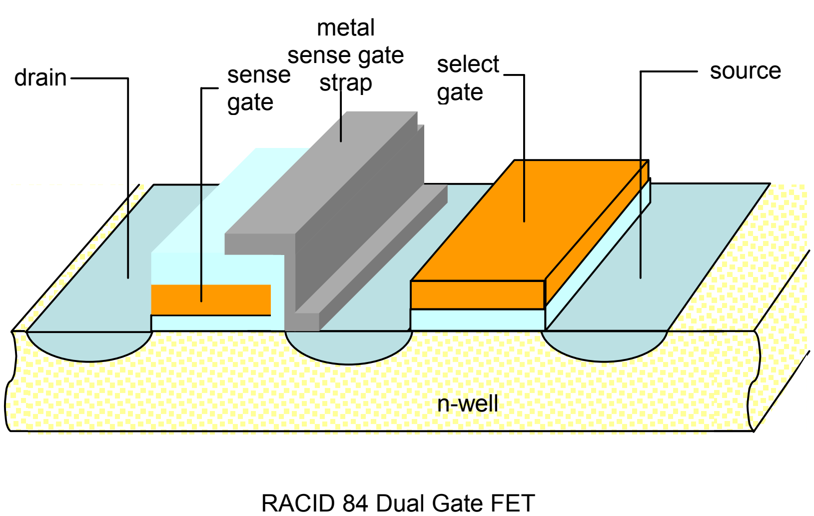

Figure 3: Dual Gate Readout FET

3. IMAGER AND CAMERA CONSTRUCTION

The RACID84/86 imagers were designed at Spectra-Physics, Cameras and Imagers. The imager design databases were sent to Supertex inc, Wafer Foundry Services, for silicon wafer fabrication. Photolithographic masks were made at Photronics, with direction from Supertex CAD and Spectra-Physics imager design groups. Wafers were fabricated on the 150-mm diameter silicon line at Supertex inc in San Jose CA.

The RACID84/86 imagers are designed for double polysilicon, double metal CMOS CID technology. Starting material is 5 ohm-cm, 28-micron thick, n-type epitaxial silicon on p-type substrates. The CMOS CID processes integrate twin-well CMOS logic circuitry with polysilicon photogate pixels built in the higher resistivity, native n-type epitaxial silicon. Active MOS photogates are made in both polysilicon layers.

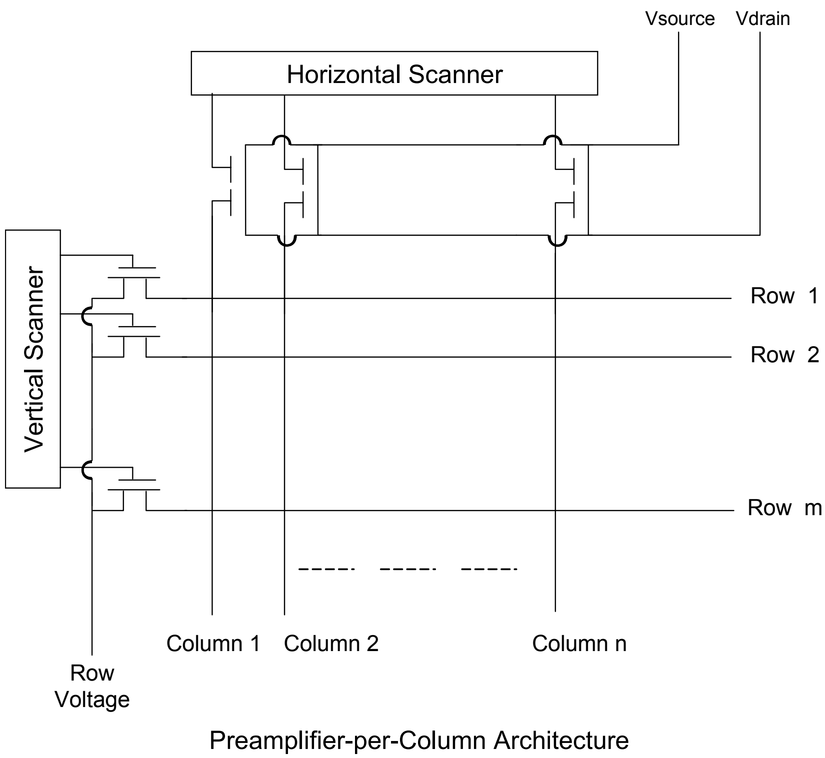

Figure 4: Preamplifier-per-Column Schematic

Borophosphosilicate glass (BPSG) reflow planarization and photoresist etchback planarization are used.

The RACID84 imager is laid out on a 2.0-micron design rule. Minimum geometries for poly 1 FET gates, contacts and vias are 2.0 microns. The 1-M pixel RACID84 imaging array is 27.7mm x 27.7mm square. The RACID84 imager die size is 32.3mm x 31.8mm. Because of the large die size, which exceeds the field size of most steppers, the RACID84 is built using the SVG700 projection aligner.

The RACID86 imager is laid out on a 1.2-micron design rule. Minimum geometries for poly 1 FET gates, contacts, and vias are 1.2 microns. The 290-K pixel RACID86 imaging array is 14.6mm x 14.6mm square. The RACID86 imager die size is 19.1mm x 18.5mm. Photolithography is done using the Canon5X stepper. To support the voltage requirements of the design, all MOSFETs on the 1.2-micron design incorporate lightly doped drain (LDD) structures. LDD spacers are removed from the pixel polysilicon photogates. SEM cross-sections of the RACID86 imager are shown in figure 8.

Imager wafers are probed at Spectra-Physics, Cameras and Imagers. SpectraCAM control electronics are integrated with custom probe cards and PENTIUM™ CPU/PC104+ computers so that 16-bit gray scale images are produced at the wafer probe workstation. Wafers with defect-free imagers are sawed and imager die are separated on the saw membrane by stretching the membrane with an underside inflation method.

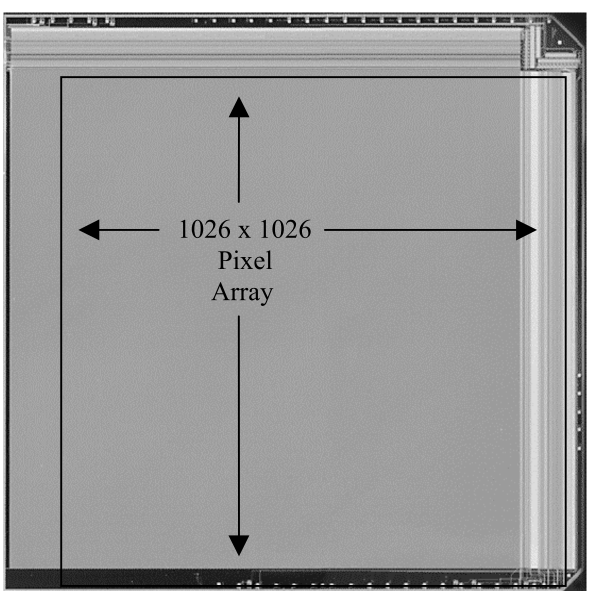

Figure 5: RACID84 imager

Imagers are attached to gold-plated ceramic substrates and wire-bonded to the imager specific interface (ISI) electronics board. The imager-ceramic unit is mounted on the three-stage thermoelectric cooler.

The SpectraCAM block diagram is shown in figure 9. In figure 10 is the expanded CAD drawing. There are five basic building blocks for the SpectraCAM camera controller: the central processing unit (CPU), the timing signal processing (TSP) board, the analog signal processing (ASP) board, the edge input/output (I/O) board, and the thermoelectric cooling dewar assembly which contains the imager. The SpectraCAM can be used in either a purged head or a sealed head configuration. The purged head SpectraCAM is pictured in figure 11. For the purged head camera, the case is anodized aluminum. The sealed head camera case is built in Kovar™.

Dark current is reduced using a three-stage bismuth-telluride thermoelectric cooler and water recirculating system. Typical imager operating temperature is -30 to -45C. At these temperatures, dark current is 6-9 carriers/pixel/second.

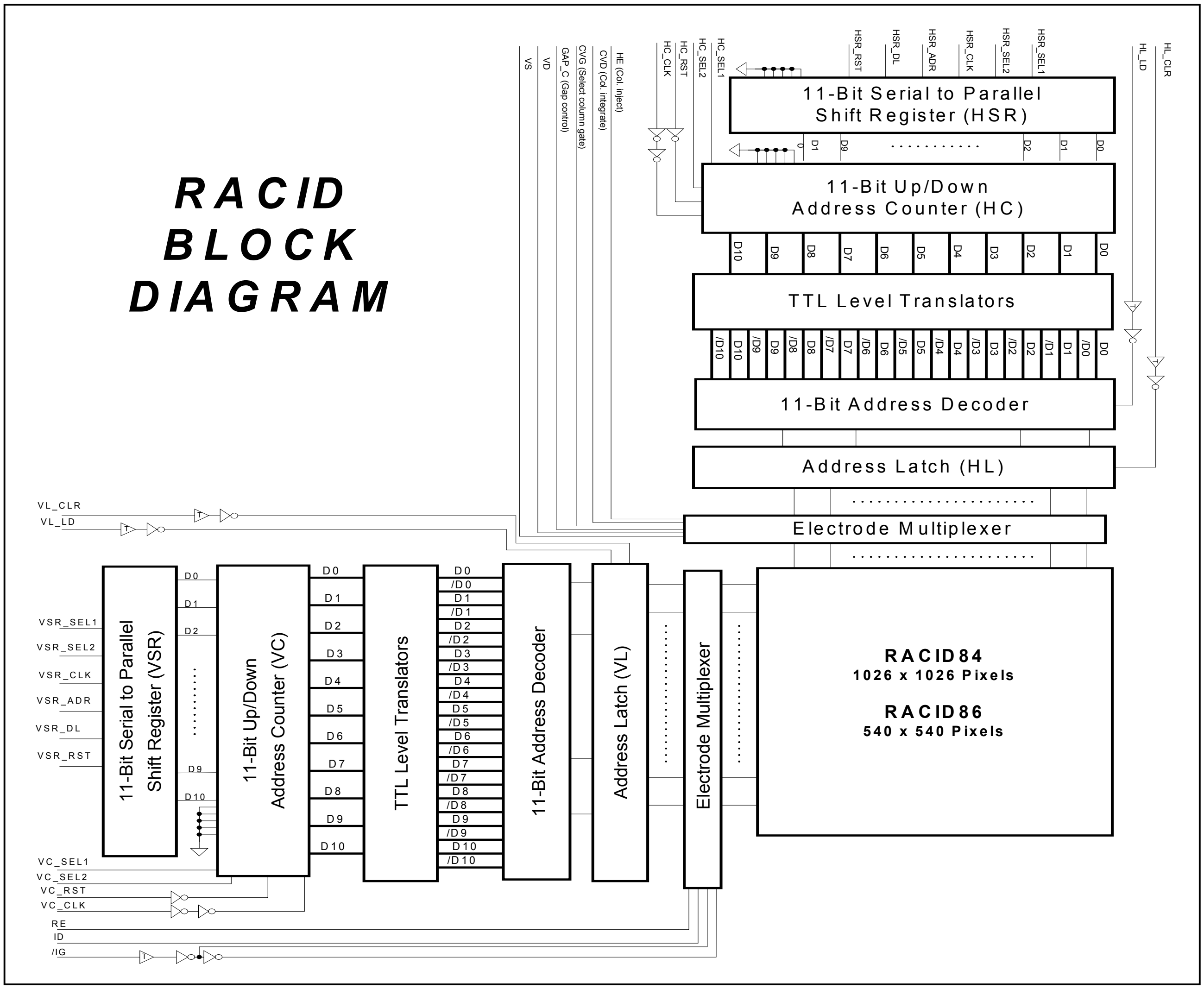

Figure 6: RACID84/86 Block Diagram

4. PERFORMANCE

The SpectraCAM84/86 responds to light from 165 nm to 1000 nm. UV/visible responsivity was measured using Oriel deuterium and tungsten light sources through a 2nm diameter aperture in an optical bench monochromator. When illuminated with the Oriel 30-watt deuterium lamp, the SpectraCAM86 UV responsivity was 100 ma/watt at 350nm and 80 ma/watt at 200 nm. The SpectraCAM84 UV responsivity was 71-89 ma/watt at 350 nm and 40-50 ma/watt at 200 nm. Responsivity and quantum efficiency curves are shown in figures 12 - 15. Quantum efficiency is calculated from the responsivity using Planck's constant.

At 50 kHz, the single read noise is typically to be 172-189 carriers for the RACID86. To date the lowest measured read noise was 135 carriers. By signal averaging with 256 non-destructive reads, the read noise is reduced to 10-11 carriers. For the flat-field 598-nm LED signal at full well amplitude, the 50 kHz single read signal-to-read noise ratio was 4K. For 256 non-destructive reads, the signal-averaged signal-to-read noise ratio was 58K. For the RACID84, the single read noise at 50 kHz was 169–304 carriers at 50 kHz. The read noise is reduced to 13-28 carriers with 256 non-destructive reads.

SpectraCAM linearity is characterized by plotting output signal vs light exposure. Using the linearity curve, the pixel full well capacity is measured from the point at which nonlinearity is 2% of full well. By this method, the RACID86 imager full well capacity is 600k carriers. Injection is the process for clearing charge from the array. Injection efficiency is characterized globally and for small segments of the pixel array. N/N+ RACID86 sample 302P060-22-10 (figure 13) showed higher responsivity than did the n/p+ samples. N/N+ global injection was less efficient than for the n/p+ samples, but adequate to meet current product needs. Pixel segment injection was inefficient. Further optimization of the n/n+ structure is needed to meet the segment inject specification for the current product.

5. APPLICATIONS

The SpectraCAM84/86 are designed for quantitative, lens-less imaging. In many scientific and industrial applications, it is important to measure photons or charged particles emitted from the subject with true spatial resolution and intensity. Due to the absorption and reflection of lens materials, particularly in the vacuum UV, it is not always possible or advantageous to use lenses.

With true random pixel access and inherent resistance to blooming, the SpectraCAM84/86 are well-suited for use as detectors in emission spectroscopy. The ability to quantify weak analyte emission lines in the presence of strong matrix emission wavelengths is critical in atomic emission spectroscopy (8). Thermo Electron (Waltham MA) has built several types of emission spectrometers using the SpectraCAM as a general purpose detector, including the IRIS Inductively Coupled Plasma – Optical Emission Spectrometer (ICP-OES) (9).

Other applications for the SpectraCAM include direct proton imaging, x-ray crystallography, and astronomy. The PMOS photogates are naturally resistant to radiation damage. By coating the RACID84/86 with lumogen, the wavelength response can be extended further into the vacuum UV with additional protection from UV radiation damage. GdO2S coatings can be used to enhance SpectraCAM response to higher energy x-rays.

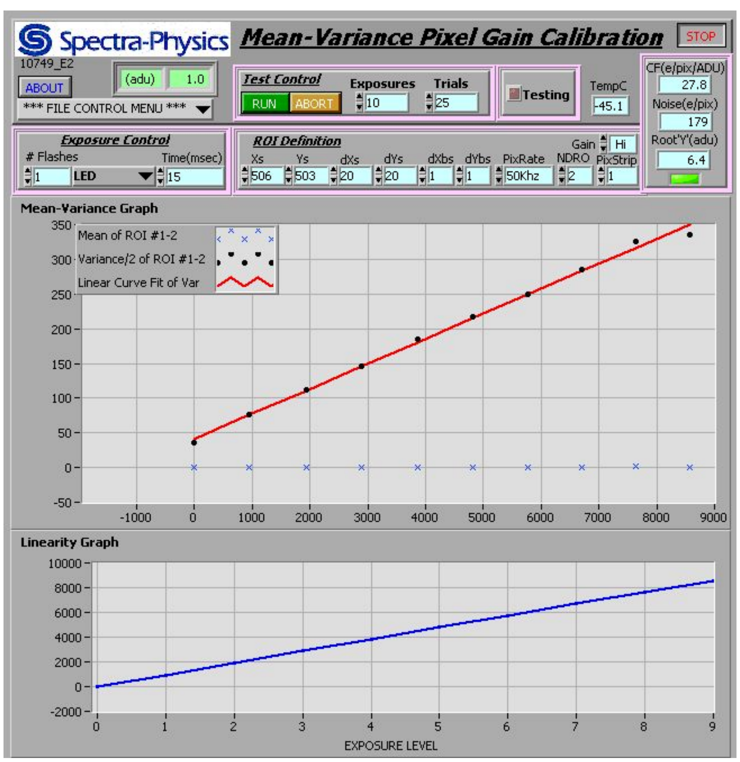

RACID Voltage Settings

VrowINJ: 4.95
VcolINJ: 4.95
VrowLO: -3.50
VrowHI: 4.60
VcolLO: 0.50
Vskim: 2.00
VcolHI: 4.70

Figure 7: SpectraCAM84 Mean Variance Plot at 50 kHz

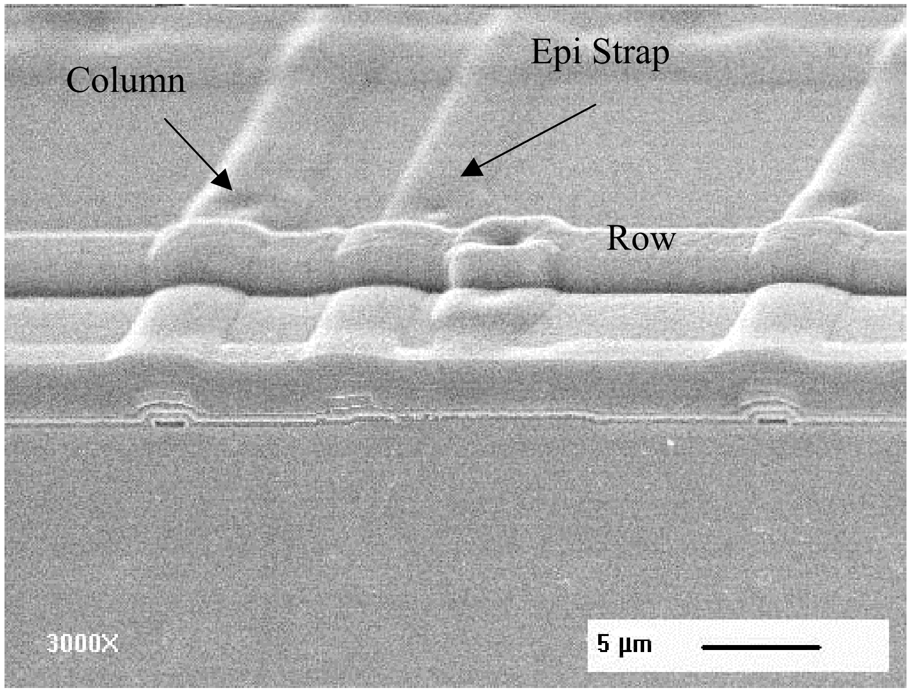

Figure 8a: SEM image of RACID86 pixel array, 1800X

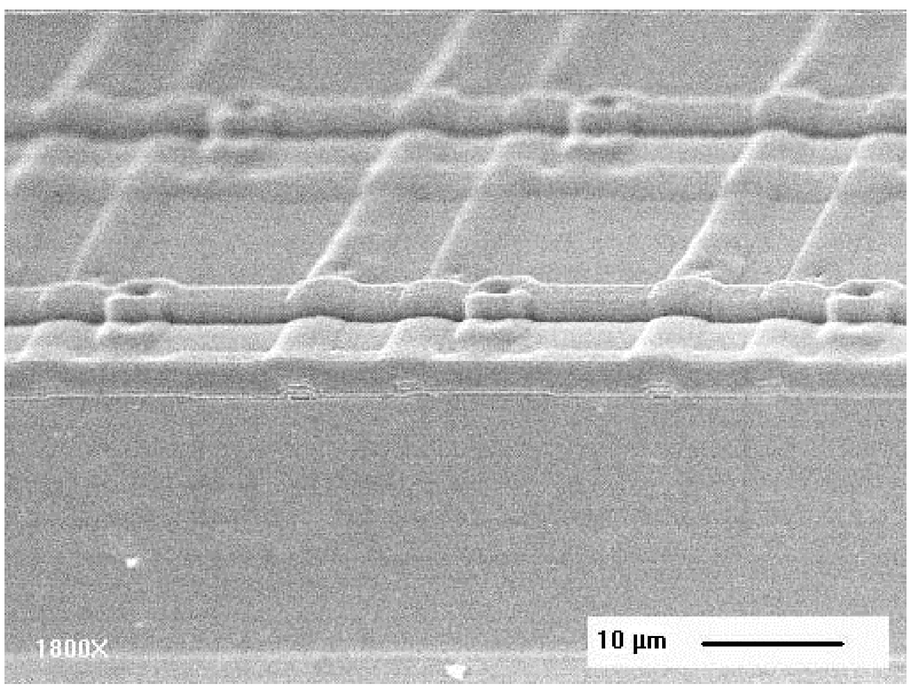

Figure 8b: SEM image of RACID86 pixel array, 3000X

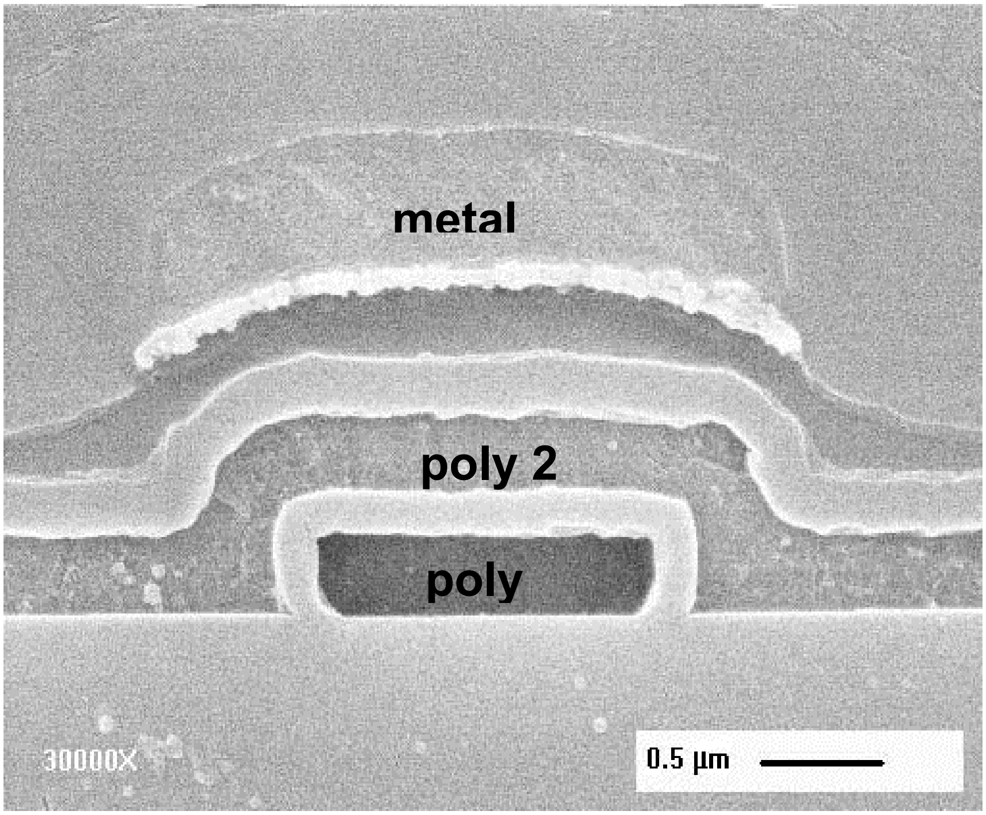

Figure 8c: SEM image of poly 2 – poly 1 overlap, RACID86 pixel, 30,000X

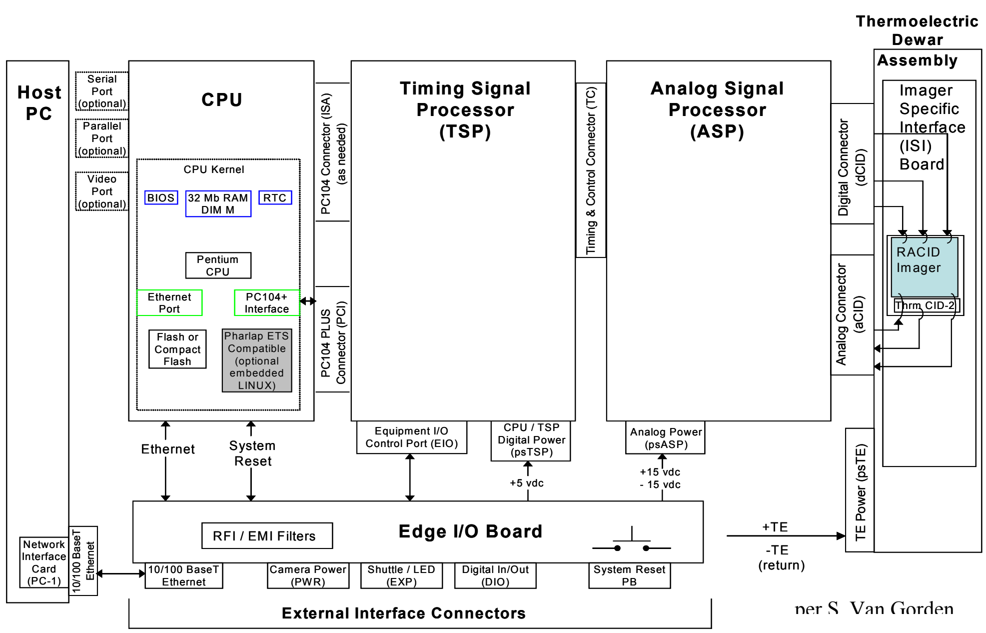

Figure 9: SpectraCAM Block Diagram

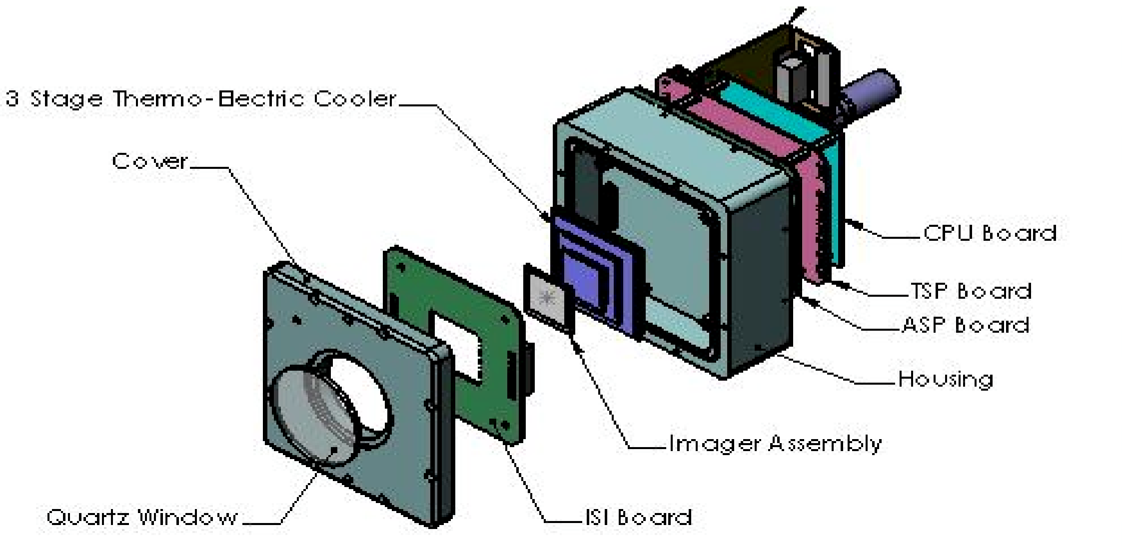

Figure 10: SpectraCAM Expanded

Figure 11: SpectraCAM86, purged camera head

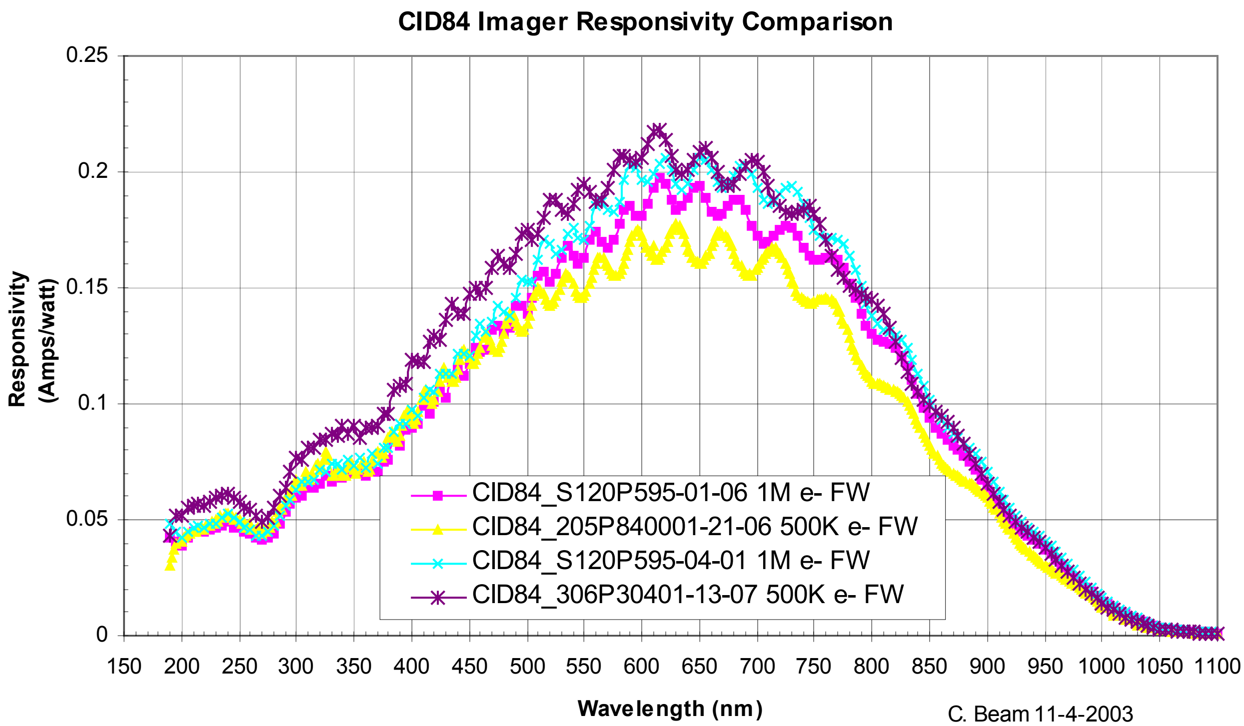

Figure 12: SpectraCAM84 Responsivity

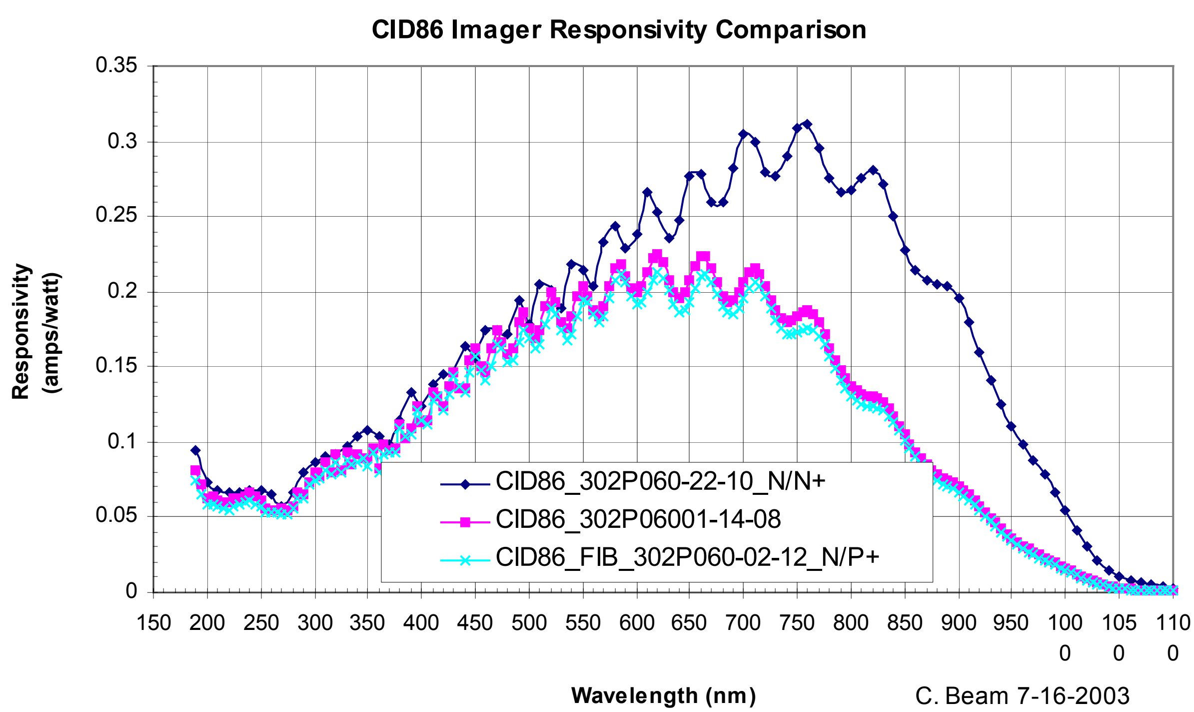

Figure 13: SpectraCAM86 Responsivity

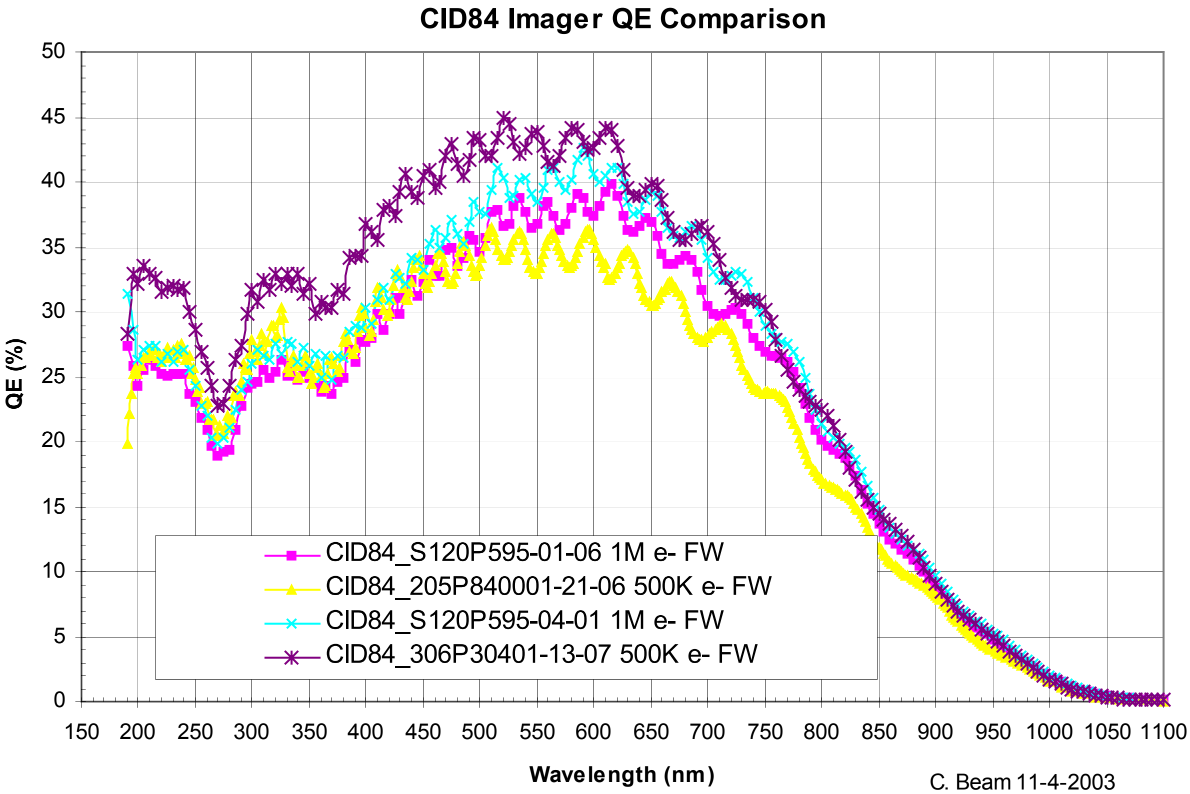

Figure 14: SpectraCAM84 Quantum Efficiency

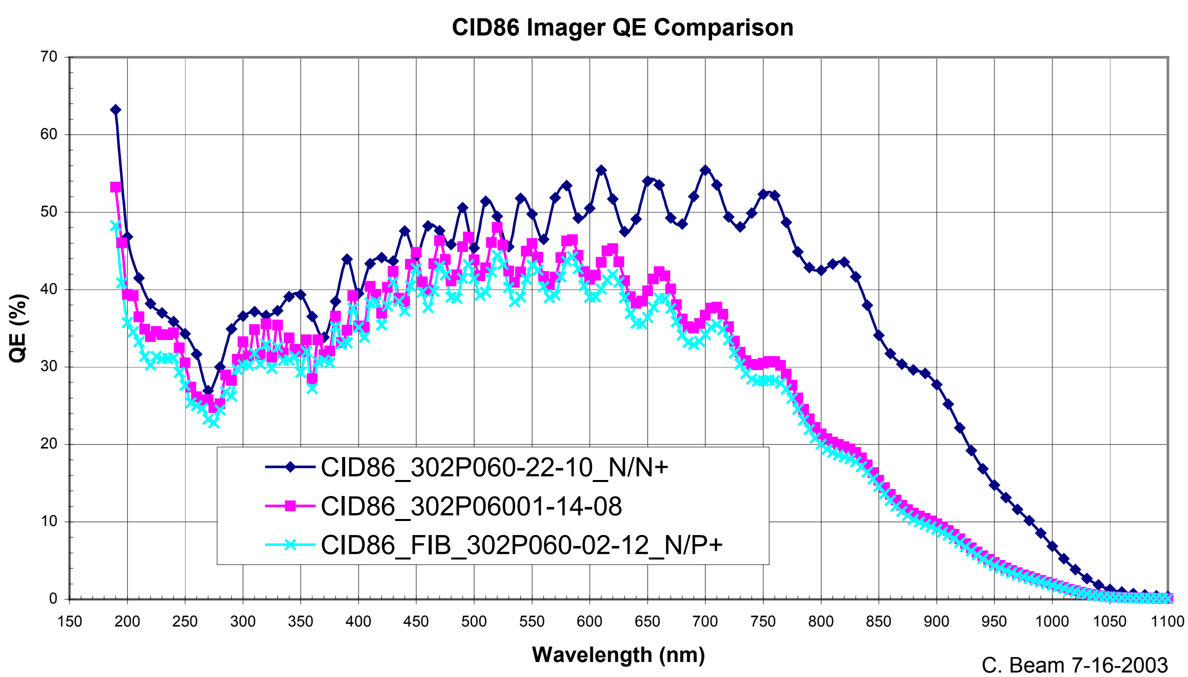

Figure 15: SpectraCAM86 Quantum Efficiency

6. ACKNOWLEDGEMENTS

This work was supported by the Thermo Electron Corporation. We thank Steve Herschbein and Larry Fischer (IBM Analytical Services) for ion beam modification of imager circuits, which aided in product development. We thank Skip Tobey, Bob Schleicher, Mike Wassall, Huw Prytherch, and the Thermo Electron SpectraCAM86 product development team for careful evaluation of RACID84/86 imagers and candid feedback. We thank Alice Everett and Sheila Escobar (Spectra-Physics) for technical support. We thank Jeff Pazak (Spectra-Physics) for support and guidance. We thank Jim Cook and Gary Sims (Spectral Instruments) for coating RACID imagers with lumogen.

7. REFERENCES

1. G. Michon, " CID Image Sensor With Improved Sensitivity," SPSE Conference on Electronic Imaging, October 13-17, 1986.
2. G. Michon, "CID Image Sensor with a Preamplifier for Each Sensing Array Row," US Patent # 4689688, 8/25/87.
3. G. Michon, "CID Image Sensor with Parallel Reading of All Cells in Each Sensing Array Row," US Patent # 4807038, 2/21/89.
4. J. Carbone, J. Hutton, F. Arnold, J. Zarnowski, S. VanGorden, M. Pilon, and M. Wadsworth, "Application of low noise CID imagers in scientific instrumentation cameras," SPIE 1447 (1991) 229-242.
5. Joseph Carbone, M. Bonner Denton, Stephen W. Czebiniak, Jeffrey J. Zarnowski, Steven N. VanGorden, Michael J. Pilon, "Collective Charge Reading and Injection in Random Access Charge Transfer Devices," US Patent # 5,717,199, 2/10/1998.
6. L. Mortara and A. Fowler, "Evaluations of charge-coupled device (CCD) performances for astronomical use," SPIE 290 Solid-State Imagers for Astronomy (1981) 28-33.
7. James Janesick, Kenneth Klaasen, and Tom Elliott, "CCD charge collection efficiency and the photon transfer technique," SPIE 570 Solid State Imaging Arrays (1985) 7-19.
8. M. Bonner Denton, Michael J. Pilon, and Jeffery S. Babis, "Vacuum Ultraviolet inductively Coupled plasma Spectroscopy for Element-Selective detection of Nonmetals," Applied Spectroscopy, **44** (1990) 975-978.
9. Michael J. Pilon, Ronald L. Stux, and Robert W. Foster, "Achieving improved optical emission spectroscopy performance through advances in charge injection device detector technology," American Laboratory, April 2000, 32-34.